RESEARCH ARTICLE

Glycolipid MPIase is essential for the TAT (twin-arginine translocation) pathway

Hanako Nishikawa, Nachi Yamamoto, Hayate Kunezaki, Yui Shirogane, Kotoka Kanno, Katsuhiro Sawasato, Miwa Yamada, Ken-ichi Nishiyama*

Department of Biological Chemistry and Food Sciences, Faculty of Agriculture, Iwate University, Morioka, Japan

eLife Assessment

This study demonstrates a critical role of the glycolipid membrane protein insertase (MPIase) in the twin-arginine translocation (TAT) pathway, a protein translocation system that is conserved across all domains of life. The successful reconstitution of the bacterial TAT system in both bacteria-derived and artificial liposomes provides **solid** experimental evidence that MPIase has a broader role in membrane protein translocation than previously recognized. By revealing the essential function of a nonproteinaceous membrane component in catalyzing a core cellular process, this work offers **fundamental** insights into the molecular mechanisms of protein translocation.

***For correspondence:** nishiyam@iwate-u.ac.jp

Competing interest: The authors declare that no competing interests exist.

Funding: See page 16

Preprint posted
09 June 2026
Sent for Review
05 June 2026
Reviewed preprint v1
30 July 2026
Reviewed preprint v2
24 September 2026
Reviewed preprint v3
13 October 2026
Version of Record
02 November 2026

Reviewing Editor: Heedeok Hong, Michigan State University, United States

© Copyright Nishikawa *et al.* This article is distributed under the terms of the Creative Commons Attribution License, which permits unrestricted use and redistribution provided that the original author and source are credited.

Abstract TAT (twin-arginine translocation) is a preprotein translocation system dedicated to membrane translocation of prefolded proteins in plants and bacteria. The TAT translocon, consisting of the TatABC subunits, drives translocation using proton motive force. However, there have been no reports on the successful reconstitution of the TAT system. In this report, we show that MPIase, a glycolipid that has been known to catalyze membrane protein integration, is essential for the TAT system. Our findings in recombinant *Escherichia coli* demonstrate that overproducing TatABC increases MPIase levels, and that depleting MPIase results in TAT precursor accumulation in the cytosol. Furthermore, co-reconstitution of MPIase with TatABC revealed the translocation activities of TAT substrates in a proton motive force-dependent manner. This is the first successful reconstitution of the TAT system and will be advantageous for understanding its mechanisms.

Introduction

The TAT (twin-arginine translocation) system, found in plant chloroplasts, bacteria, and mitochondria of some protozoa and plants, is dedicated to the membrane translocation of presecretory proteins with a TAT signal sequence (***Chaddock et al., 1995***; ***Mould and Robinson, 1991***; ***Berks, 2015***; ***Wu et al., 2000***). This signal sequence is composed of three regions, *n*, *h*, and *c* regions from N-terminus. The *n* region contains the consensus motif of 'SRRxFLK', which includes the consecutive twin arginine residues that are essential for TAT translocation (***Berks, 1996***). The central *h* region (hydrophobic region) of the TAT signal sequence is on average less hydrophobic than that of the Sec signal sequence (***Cristóbal et al., 1999***). The *c* region of the TAT signal sequence often contains basic amino acids that have been shown to function as a Sec-avoidance motif (***Blaudeck et al., 2003***), preventing recognition of the TAT substrates by the Sec pathway (***Bogsch et al., 1997***). This region contains a cleavage site by Lep. Unlike the presecretory proteins that are translocated through the SecYEG or Sec61 translocon, TAT substrates maintain their folded structures during translocation. In many cases, TAT substrates fold and are transported with specific cofactors (***Berks, 1996***; ***Palmer et al., 2005***). It is known that *Escherichia coli* K12 possesses 27 TAT substrates (***Palmer et al., 2005***). TAT substrates

are translocated through the translocation machinery formed by TatABC using the proton motive force (PMF) as the driving force (**Mould and Robinson, 1991**; **Yahr and Wickner, 2001**; **Bageshwar and Musser, 2007**; **Zhou et al., 2023**). The TAT machinery consists of the TatA and TatC families, all of which are membrane proteins (**De Leeuw et al., 2001**). In *E. coli*, the TatA family includes TatA and TatB, as well as TatE (**Sargent et al., 1998**; **Weiner et al., 1998**; **Bogsch et al., 1998**). TatE is a functional homologue of TatA that is not essential for TAT translocation (**Sargent et al., 1998**; **Jack et al., 2001**). TatA and TatB are structurally similar but functionally distinct, since both are essential for TAT translocation (**Sargent et al., 1999**; **Hicks et al., 2003**; **Yen et al., 2002**). On the other hand, TatA and TatE have overlapping functions in the TAT system (**Sargent et al., 1998**). All three proteins are integral membrane proteins containing a single transmembrane helix (TMH), followed by a cytoplasmic amphipathic helix (APH) **Walther et al., 2010**; **Rodriguez et al., 2013**. TatC is a polytopic membrane protein with six TMHs (**Rollauer et al., 2012**; **Ramasamy et al., 2013**). TatC forms a complex with TatB at an equal molar ratio, which recognizes the signal peptides of TAT substrates **Bolhuis et al., 2001**; **Cline and Mori, 2001**; **de Leeuw et al., 2002**; **Alami et al., 2003**; **Richter and Brüser, 2005**; **Tarry et al., 2009**. In contrast, TatA forms a homomultimer that associates with the TatBC complex with different stoichiometries depending on the size of the substrate (**Rodriguez et al., 2013**; **Dabney-Smith and Cline, 2009**; **Leake et al., 2008**; **Gohlke et al., 2005**; **Beck et al., 2013**; **McDevitt et al., 2006**; **Oates et al., 2005**). It is also reported that a signal peptide alone can induce TatA multimerization (**Dabney-Smith and Cline, 2009**). Binding of substrates to the TatBC complex causes TatA to assemble around the complex in a PMF-dependent manner (**Alami et al., 2003**; **Mori and Cline, 2002**). The TatA cluster then forms a translocon through which the TAT substrates can pass when bound to the TatBC complex (**Alami et al., 2003**; **Mori and Cline, 2002**; **Alcock et al., 2013**; **Rose et al., 2013**; **Dabney-Smith et al., 2006**). According to MD simulations, the short TMHs and APHs of the TatA cluster have been shown to thin the membranes, thereby destabilizing the lipid bilayer of the cell membranes and allowing the translocation of prefolded proteins (**Brüser and Sanders, 2003**; **Mehner-Breitfeld et al., 2022**). Once translocation is complete, the substrate is released from the TatABC complex, and the signal sequence is cleaved by membrane-located leader peptidase (**Yahr and Wickner, 2001**; **Lüke et al., 2009**). Assembly of the TAT machinery is a transient process that occurs exclusively during substrate translocation (**Mori and Cline, 2002**; **Cline and McCaffery, 2007**). As mentioned above, extensive studies performed by numerous researchers have significantly advanced our understanding of the molecular mechanisms underlying the TAT system, particularly following the identification of a Tat component in 1977 (**Settles et al., 1997**). However, a reconstitution system for the TAT pathway has yet to be reported. Therefore, we hypothesized that a missing piece is necessary for successfully reconstituting the TAT system.

MPIase (*M*embrane *P*rotein *I*ntegr*ase*) is a glycolipid that catalyzes the integration of membrane proteins (**Nishiyama et al., 2012**). Its glycan chain consists of approximately 10 repeats of three *N*-acetylated amino sugars and is linked to diacylglycerol (DAG) by a pyrophosphate linker (**Nishiyama et al., 2012**; **Figure 1—figure supplement 1**). This glycan chain has a molecular chaperon-like function, that is the glycan interacts directly with the substrate membrane proteins prior to insertion to prevent aggregation (**Nishiyama et al., 2012**; **Mori et al., 2022**; **Fujikawa et al., 2023**). The glycan is flexible on the membrane surface **Nomura et al., 2019**. DAG in the membrane bilayer blocks the disordered, spontaneous insertion by reducing the mobility of the acyl chain within the bilayers, while MPIase restores the mobility, allowing insertion with the substrate binding (**Nomura et al., 2019**). In combination with the pyrophosphate linker, MPIase perturbs the membrane structure, enabling membrane proteins to insert into membranes. The negatively charged pyrophosphate of MPIase also attracts the positive charges near the TMH of the substrates (**Mori et al., 2022**; **Fujikawa et al., 2023**).

MPIase can drive the membrane insertion of simple membrane proteins with a single TMH. MPIase also acts cooperatively with proteinaceous factors responsible for membrane insertion, such as the SecYEG translocase and the YidC insertase, in both Sec-dependent and -independent membrane insertion (**Nishiyama et al., 2010**; **Nishikawa et al., 2017**). MPIase is co-purified with SecYEG (**Moser et al., 2013**) and YidC (**Endo et al., 2022**), indicating that MPIase interacts with these proteins directly. MPIase also stimulates protein translocation by affecting the dimer structure of SecYEG (**Moser et al., 2013**; **Nishiyama et al., 1996**; **Nishiyama et al., 2006**). Thus, MPIase is generally involved in both membrane integration and translocation (**Nishikawa et al., 2022**; **Sasaki et al., 2019**), leading us to hypothesize that MPIase is also involved in the TAT pathway.

Results

MPIase is involved in the TAT pathway in vivo

Recently, we found that CdsA and its paralogue YnbB, CDP-DAG synthases, are involved in MPIase biosynthesis and constructed the strain KS23 (Δ*cdsA*::*cat*Δ*ynbB*) in which both the *cdsA* and *ynbB* genes were disrupted (***Sawasato et al., 2019a***). The expression level of MPIase in this strain can be controlled by the addition of arabinose, since the *cdsA* gene is placed under the control of the *araBAD* promoter on a low-copy plasmid (pAra-CdsA). When arabinose is removed from the culture, MPIase becomes depleted ('ΔMPIase' conditions; ***Sawasato et al., 2019a***). We investigated the effect of MPIase depletion on the TAT pathway by using KS23/pAra-CdsA and its parent strain (EK413; ***Figure 1***). When the TAT substrate SufI was expressed in EK413, the signal sequence-cleaved mature form of the protein was observed, in addition to the precursor. The level of the mature form increased when TatABC was provided from the *tet* promoter on a plasmid (pTet-TatABC) in addition to chromosomal expression. This finding is consistent with a previous report (***Alami et al., 2002***). The amount of mature SufI did not change upon SufI induction, indicating that the level was saturated. A large part of untranslocated precursors was aggregated (***Figure 1—figure supplement 2***). In marked contrast, no mature form was observed upon MPIase depletion in KS23/pAra-CdsA, even when TatABC was expressed from pTet-TatABC (***Figure 1A***, top). Upon SufI induction, a smaller band marked by a star appeared in addition to the precursor; however, this band is likely a degradation product of the precursor that had not been translocated, as it is larger than the mature band. The addition of arabinose restored MPIase expression (***Figure 1A***, middle left) and generated the mature form of SufI (***Figure 1A***, top). These results strongly suggest that MPIase is involved in TAT translocation. Similar results were obtained when using TorA, another TAT substrate: no mature form was observed upon MPIase depletion (***Figure 1A***, bottom left). The low level of TAT substrates under the MPIase depletion is due to the fact that MPIase-depleted cells hardly proliferate. Although TorA translocation appears to be less efficient than SufI translocation, this might be because TorA's folding efficiency is lower in the absence of trimethylamine N-oxide (TMAO), as previously reported (***Santini et al., 1998***). TatABC, which had been expressed prior to arabinose removal, was still present after MPIase depletion (see ***Figure 2C***). To confirm that the processing to the mature form represents the TAT translocation, we examined the TAT signal mutants SufI (KK; ***Figure 1A***, middle right) and TorA (KK; ***Figure 1A***, bottom right). In these mutants, the twin arginine residues in the signal sequence were replaced with twin lysine residues, resulting in an inability to translocate across the IM. We observed that these KK mutants did not convert to the mature form, even in TatABC-overproducing strains (***Figure 1A***, middle). These results indicate that the TAT translocation was properly studied. We investigated the involvement of MPIase in more detail using pulse-chase experiments (***Figure 1B***). To facilitate TAT translocation, TatABC was overexpressed from the *tac* promoter on a plasmid (pTac-TatABC). In the wild-type strain harboring pTac-TatABC (***Figure 1B***, top left), the precursor form of SufI was efficiently converted to the mature form. No mature form was observed when the signal mutant SufI (KK) was used (***Figure 1B***, top right), confirming that the TAT translocation was analyzed correctly. When MPIase was depleted, no mature form was observed even after a 10 min chase (***Figure 1B***, bottom, 'ΔMPIase'), confirming MPIase's involvement in the TAT system. When MPIase synthesis was induced (***Figure 1B***, bottom, '+MPIase'), the mature form appeared, but the conversion rate was much slower than under wild-type conditions. The reason for this will be discussed later. To investigate the role of MPIase in the TAT system, we performed cell fractionation into periplasmic and spheroplast fractions (***Figure 1C***). When the MPIase-depleted strain expressing TatABC and SufI was fractionated, the precursor was recovered in the spheroplast fraction, and no mature form was observed. This indicates that SufI was not translocated (***Figure 1C***, left, 'ΔMPIase'). Conversely, mature SufI was translocated to the periplasm when MPIase was expressed (***Figure 1C***, left, '+MPIase'). Successful fractionation was confirmed by detecting the periplasmic protein β-lactamase and the cytoplasmic protein SecB. Similar results were obtained when TorA-GFP, in which the TorA signal is connected to GFP, was examined (***Figure 1C***, right), confirming that TorA-GFP is not translocated upon MPIase depletion. These cells expressing TorA-GFP were also used to detect the subcellular localization directly by monitoring its fluorescence (***Figure 1D***). In the presence of MPIase, the envelope fraction exhibited green fluorescence, indicating that GFP is localized in the periplasm or on the inner membrane at least (left). Conversely, in the absence of MPIase, the entire cell exhibited uniform fluorescence, indicating that TorA-GFP is localized in the cytoplasm under these conditions (right). These results are consistent with

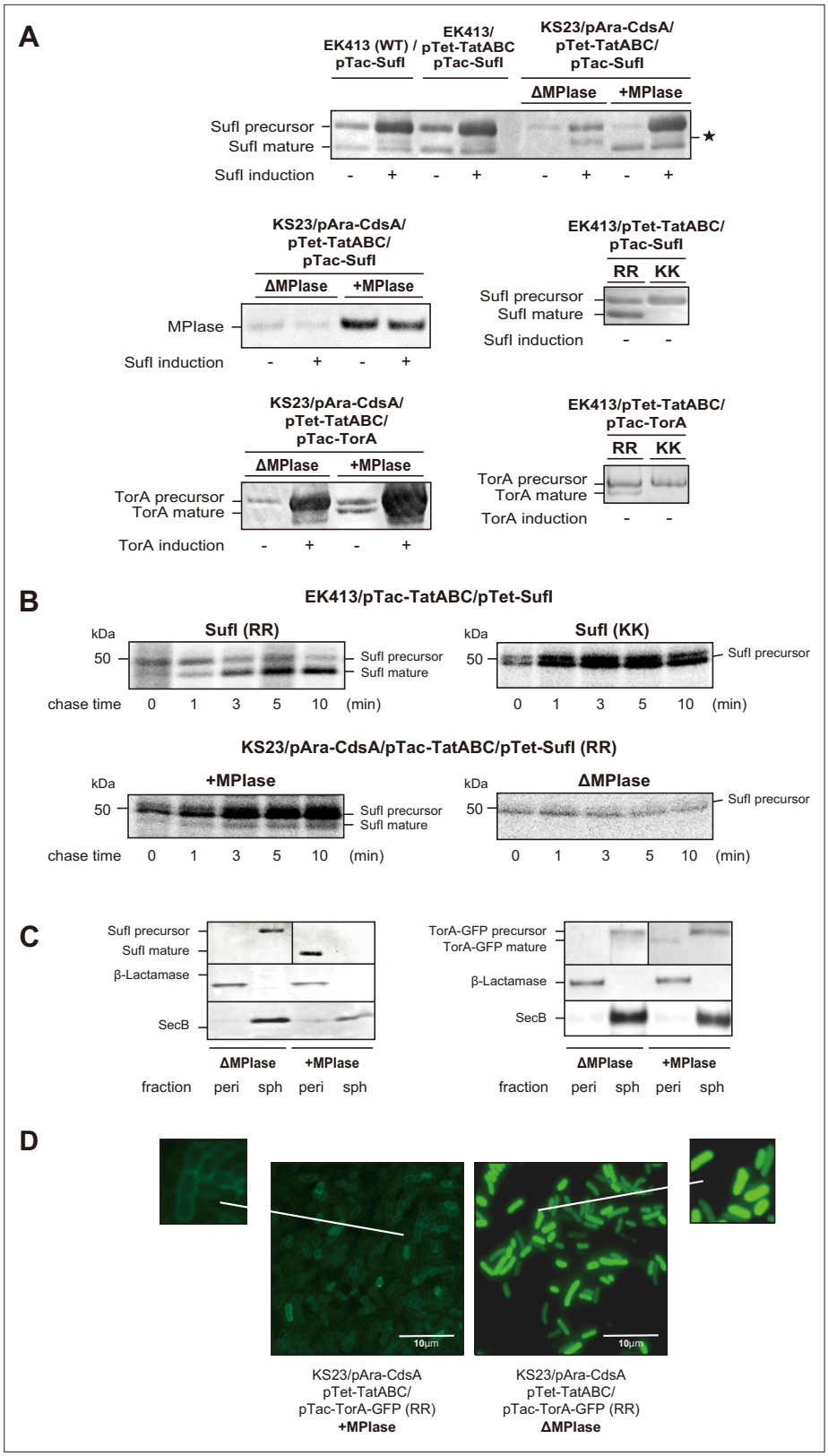


Figure 1. MPIase depletion causes the accumulation of TAT substrate precursors. (**A**) Detection of SufI and TorA precursors upon MPIase depletion. SufI (top) and TorA (bottom) were expressed in the indicated strains. IPTG (1 mM) was added at early log phase, and cultivation was continued for 2 hr. The cells were subjected to TCA precipitation, followed by SDS-PAGE/immunoblotting. The precursor and mature forms were then detected as

Figure 1 continued on next page

Figure 1 continued

indicated. MPIase depletion was confirmed in KS23 (middle left). Defects in the processing of SufI (middle right) and TorA (bottom right) with the KK signal were also confirmed. The symbol '' denotes degradation products of the SufI precursor. (**B**) Pulse-chase experiments of SufI processing after MPIase depletion. EK413/pTac-TatABC harboring pTet-SufI(RR) (top left) or pTet-SufI(KK) (top right), and KS23/pAra-CdsA/pTac-TatABC harboring pTet-SufI(RR) (+MPIase; bottom left, ΔMPIase; bottom right) were pulse-labeled for 30 s and then chased for the indicated periods. SufI(RR) and SufI(KK) were isolated using the attached His tags, followed by SDS-PAGE/autoradiography. (**C**) Subcellular localization of SufI and TorA-GFP after MPIase depletion. KS23/pTet-TatABC/pTac-SufI(RR) (left) and KS23/pTet-TatABC/pTac-TorA-GFP(RR) (right) were cultivated in the presence (+MPIase) or absence (ΔMPIase) of arabinose. The TAT substrates were leaky expressed from the *tac* promoter. The cells were then fractionated into periplasmic (peri) and spheroplast (sph) fractions. The indicated proteins were detected by immunoblotting. (**D**) Subcellular localization of TorA-GFP after MPIase depletion as revealed by fluorescence microscopy. The indicated strains were cultivated, TorA-GFP was induced, and then it was observed by fluorescence microscopy. The scale bars represent 10 μm. A magnified view of part of the '+MPIase' sample is shown on the left.

The online version of this article includes the following source data and figure supplement(s) for figure 1:

Source data 1. PDF file containing original immunoblots and autoradiographs for ***Figure 1***, indicating the relevant bands and treatments.

Source data 2. Original files for immunoblot and pulse-chase analysis displayed in ***Figure 1***.

Figure supplement 1. Structure of MPIase.

Figure supplement 2. The level of inclusion bodies of TAT substrates.

Figure supplement 2—source data 1. PDF file containing original immunoblots for ***Figure 1—figure supplement 2***, indicating the relevant bands and treatments.

Figure supplement 2—source data 2. Original files for immunoblot analysis displayed in ***Figure 1—figure supplement 2***.

those of the subcellular fractionation (see ***Figure 1C***). Taken together, we conclude that MPIase is involved in the TAT system in vivo.

Upregulation of MPIase upon TatABC overproduction is essential for in vitro TAT translocation

The TAT pathway can be reproduced in vitro using inverted membrane vesicles (INV), as depicted in ***Figure 2—figure supplement 1***. However, it has been shown that overproduction of TatABC is necessary for translocation into INV (***Yahr and Wickner, 2001***; ***Alami et al., 2002***). To reproduce these observations, we prepared INV from wild-type strains with an empty vector (***Figure 2A***, BL21/pT7 (empty)) and from TatABC-overproducing strains (***Figure 2A***, BL21/pT7-TatABC), which were then subjected to the SufI translocation assay in vitro. TatABC overproduction with this vector was confirmed by immunoblotting (***Figure 2—figure supplement 2***). As reported (***Yahr and Wickner, 2001***; ***Alami et al., 2002***), SufI translocation into INV was observed only when TatABC was overproduced (***Figure 2A***, top left). In the absence of INV, SufI was completely digested by PK (-). These results indicate that SufI is translocated in a TatABC-dependent manner. SufI (KK) was not translocated, even when TatABC-overproducing INV were used (***Figure 2A***, top right), indicating that the TAT pathway is adequately analyzed in our experimental system. We observed the same trend with another TAT substrate, TorA-GFP (***Figure 2A***, bottom). To further test the involvement of MPIase in the TAT pathway in this in vitro system, we used a *cdsA*/*ynbB* knockout strain with a BL21 (DE3) background (KS46) harboring pAra-CdsA. We then prepared MPIase-depleted INV with TatABC overproduction, followed by SufI translocation (***Figure 2B***). Since TatABC was overproduced prior to MPIase depletion, these INV contain the overproduced amount of TatABC (***Figure 2C***) but not MPIase (***Figure 2D***). We observed that SufI was not translocated into these MPIase-depleted INV, which further supports the involvement of MPIase. Consistently, the anti-MPIase antibody inhibited SufI translocation (***Figure 2—figure supplement 3***). However, we also found that the translocation activity with MPIase-induced INV (***Figure 2B***, '+MPIase') did not recover to the level observed with the wild-type INV with TatABC overproduction (***Figure 2B***, 'BL21/pT7-TatABC'). The reason for the incomplete recovery was that TatABC overproduction caused MPIase upregulation (***Figure 2D***). Significant MPIase upregulation occurred when TatABC overproduction was induced in BL21(DE3). However,

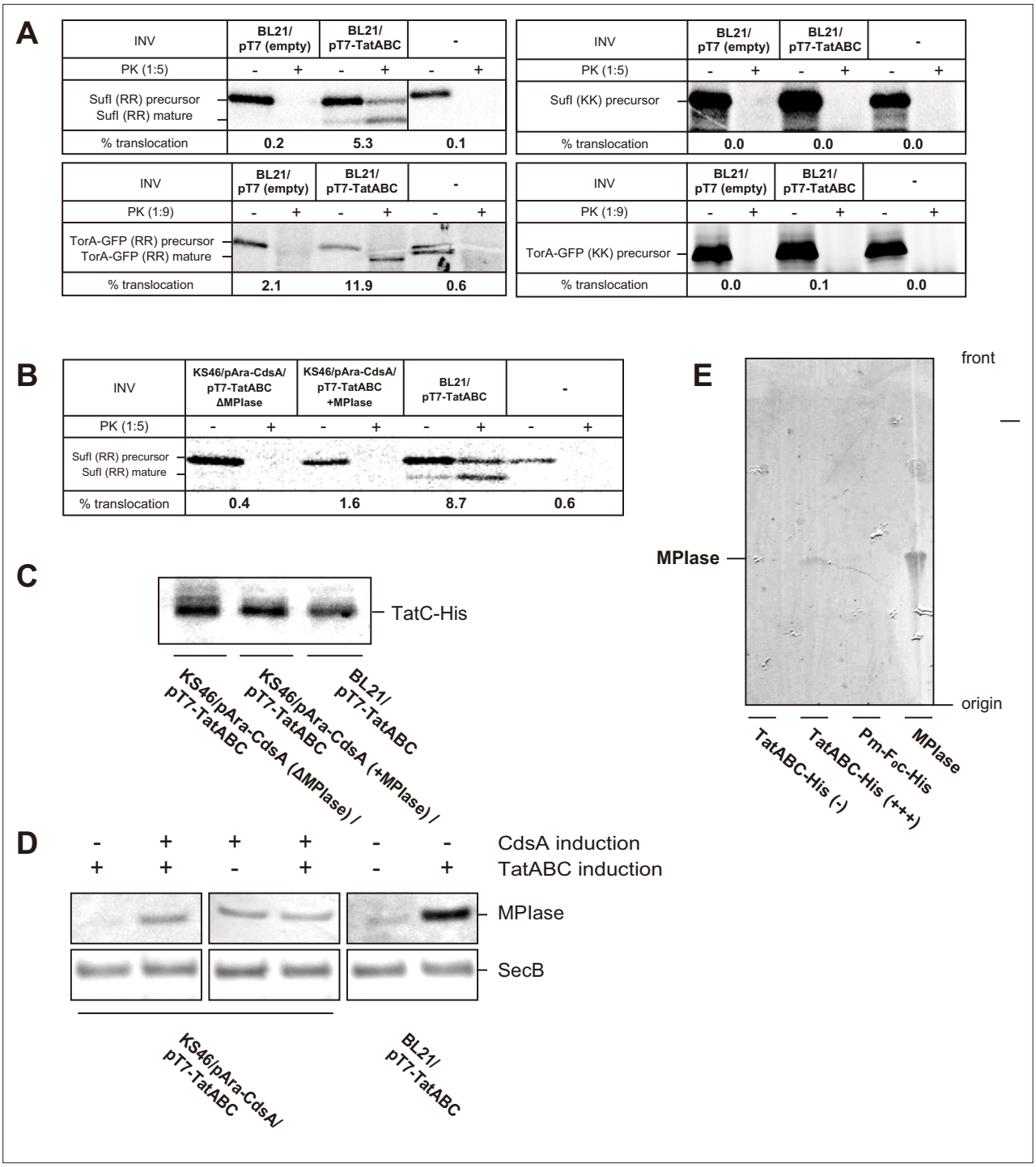


Figure 2. TAT substrates are translocated into INV in vitro when TatABC and MPIase are both overproduced. (**A**) Translocation of SufI and TorA-GFP into TatABC-overproducing INV. SufI (top) and TorA-GFP (bottom) were synthesized in vitro in the presence of INV prepared from the indicated strains. INV was omitted in the '-' samples. The signal sequences on the left are wild-type (RR), while the sequences on the right are mutants (KK). Translocated materials were generated after PK digestion (+). One-fifth of the reaction mixture was analyzed as the translation standard (-). Translocation activities, expressed as a percentage of the amount of the synthesized proteins, are shown at the bottom of each autoradiogram. (**B**) Depletion of MPIase resulted in the failure of TAT translocation. INV were prepared from KS46/pAra-CdsA harboring pT7-TatABC, which was cultivated in the presence (+MPIase) or absence (ΔMPIase) of arabinose. After washing arabinose, IPTG was added at 1 mM to induce TatABC, and cultivation was continued for 2 hr prior to INV preparation. SufI translocation was then performed as described in (**A**). (**C**) The level of TatC in INV used in (**A**) and (**B**). Each INV (10 μg) was analyzed by SDS-PAGE, followed by immunoblotting using anti-RpmJ-His antibodies. The position of TatC-His was shown. (**D**) MPIase is upregulated upon TatABC overproduction. The expression levels of MPIase in the strains used in (**B**) were determined by immunoblotting. CdsA and TatABC were

Figure 2 continued on next page

Figure 2 continued

induced as indicated. SecB levels were determined as a loading control. (**E**) MPIase is co-purified with TatABC. INV prepared from BL21/pT7-TatABC-His induced with 1 mM IPTG (+++) or not induced (-), and BL21/pT7-Pm-F_0b-His induced with 1 mM IPTG, solubilized with DDM, were applied to a TALON column, then eluted. The eluates were analyzed by TLC, followed by immunodetection of MPIase. The positions of the origin/front and MPIase are shown. Purified MPIase was also analyzed at right.

The online version of this article includes the following source data and figure supplement(s) for figure 2:

Source data 1. PDF file containing original immunoblots and autoradiographs for ***Figure 2***, indicating the relevant bands and treatments.

Source data 2. Original files for immunoblot and translocation analysis displayed in ***Figure 2***.

Figure supplement 1. Schematic diagram of the in vitro protein translocation assay system using INV or proteoliposomes.

Figure supplement 2. Expression levels of TatA in the INV used in ***Figure 2A***.

Figure supplement 2—source data 1. PDF file containing original immunoblots for ***Figure 2—figure supplement 2***, indicating the relevant bands and treatments.

Figure supplement 2—source data 2. Original files for immunoblot analysis displayed in ***Figure 2—figure supplement 2***.

Figure supplement 3. The anti-MPIase antibody inhibits SufI translocation into TatABC-overexpressed INV.

Figure supplement 3—source data 1. PDF file containing original autoradiograms for ***Figure 2—figure supplement 3***, indicating the relevant bands and treatments.

Figure supplement 3—source data 2. Original files for translocation analysis displayed in ***Figure 2—figure supplement 3***.

Figure supplement 4. SecYEG overproduction does not induce MPIase upregulation.

Figure supplement 4—source data 1. PDF file containing original immunoblots for ***Figure 2—figure supplement 4***, indicating the relevant bands and treatments.

Figure supplement 4—source data 2. Original files for immunoblot analysis displayed in ***Figure 2—figure supplement 4***.

Figure supplement 5. Purification of Pm-F_0b and TatABC.

Figure supplement 5—source data 1. PDF file containing original Coomassie Brilliant Blue-stained gels for ***Figure 2—figure supplement 5***, indicating the relevant bands and treatments.

Figure supplement 5—source data 2. Original files for gels displayed in ***Figure 2—figure supplement 5***.

MPIase expression remained unchanged with TatABC overproduction in KS46, in which *cdsA* was induced from the plasmid pAra-CdsA (***Figure 2D***). Therefore, authentic promoters for *cdsA* should be responsible for this upregulation, because CdsA is a rate-limiting enzyme for MPIase biosynthesis (***Sawasato et al., 2019a***). Since the levels of Tat components in BL21(DE3) and KS46/pAra-CdsA grown with arabinose were similar (***Figure 2C***), it is reasonable to conclude that MPIase upregulation is necessary for the translocation activity in vitro of the TAT pathway into INV. This explains the low activity of MPIase-induced INV (***Figure 2B***, 'KS46/pAra-CdsA +MPIase'). These results are consistent with the fact that the SufI translocation was not fully restored in the pulse-chase experiments when MPIase was induced from pAra-CdsA (see ***Figure 1B***). MPIase upregulation was specific to TatABC overproduction; MPIase levels were barely affected by SecYEG overproduction (***Moser et al., 2013***; ***Figure 2—figure supplement 4***). These results strongly suggest that TatABC and MPIase function cooperatively. To examine whether the interaction between TatABC and MPIase is direct and physical, we detected MPIase in the TatABC-His preparation purified via metal affinity chromatography. As shown in ***Figure 2E***, MPIase was co-purified with TatABC. Furthermore, the amount of MPIase precipitated with TatABC increased significantly with TatABC overproduction (***Figure 2E***). When His-tagged F_0b from *Propionigenium modestum* (Pm-F_0b-His) was expressed and used as a control, no detectable amount of MPIase was precipitated. Under these conditions, both TatABC-His and Pm-F_0b-His were purified to homogeneity (***Figure 2—figure supplement 5***). These results indicate that TatABC and MPIase directly and specifically interact with each other. Based on these results, we concluded that the TatABC requires MPIase to function.

MPIase is the missing piece for successfully reconstituting the TAT pathway

Results obtained thus far, both in vivo and in vitro, demonstrate the essentiality of both TatABC and MPIase. Therefore, we assumed that the TAT reconstitution might be possible if TatABC and MPIase were both present and PMF was imposed. To test if our reconstitution system would work, we started

with a crude system using proteoliposomes reconstituted from the solubilized membranes. First, we prepared proteoliposomes from solubilized membranes with overproduced amounts of TatABC and purified F_0F_1-ATPase from thermophilic bacteria (see ***Figure 3B***, left), followed by inclusion of DAG for stable generation of PMF (***Stiegler et al., 2011***). However, these proteoliposomes were inactive with regard to SufI translocation (***Figure 3A***, top left, '+PL/DAG'). We found that fusing MPIase-containing liposomes to the proteoliposomes greatly enhanced SufI translocation (***Figure 3A***, top left, '+PL/DAG/MPIase'). This may be because MPIase was not efficiently recovered in the proteoliposome fraction due to the hydrophilic nature of MPIase's glycan moiety (***Nishiyama et al., 2012***). These results again indicate that MPIase is essential for the TAT system. Here, we could not observe the signal sequence processing. This may be due to the dilution of membrane proteins, including Lep, in proteoliposome membranes since signal cleavage and translocation are not coupled (***Rose et al., 2013***). Even when MPIase-containing liposomes were fused, SufI (KK) was not translocated into the proteoliposomes (***Figure 3A***, bottom left). We also examined the post-translational translocation using a partially purified SufI precursor (***Figure 3A***, top right). We observed SufI (RR) translocation into TatABC/MPIase proteoliposomes in an ATP-dependent manner (i.e. a PMF-dependent manner), but not SufI (KK) translocation. Thus, the TAT reconstitution was achieved through a combination of TatABC, MPIase, and F_0F_1-ATPase.

Next, we purified TatA, TatB, and TatC individually through an attached His tag (***Figure 3B***, right). We confirmed that expressing each His-tagged TatA, TatB, and TatC complemented the SDS-sensitive phenotype of the corresponding knockout strain (***Figure 3—figure supplement 1***). Using these purified proteins, we reconstituted proteoliposomes containing TatABC and F_0F_1-ATPase. Then, we fused them with MPIase/DAG liposomes. The TatABC-MPIase proteoliposomes containing F_0F_1-ATPase exhibited activity with respect to SufI translocation (***Figure 3C***, left). This activity was comparable to that of proteoliposomes reconstituted with solubilized membranes (***Figure 3A***). On the other hand, SufI (KK) was not translocated into the proteoliposomes (right). In these experiments, reconstituted proteoliposomes were prepared using a TatA/B/C weight ratio of 1/1/1. To obtain higher activity, we examined various TatA/B/C ratios. We found that increasing the amount of TatA gave slightly higher activity. We then prepared proteoliposomes containing TatA/B/C at a ratio of 10/1/1. Similar results with improved activity were obtained when using TorA-GFP (***Figure 3D***). Proteoliposomes containing both TatABC and MPIase allowed for the translocation of TorA-GFP (RR) but not TorA-GFP (KK). The translocation of TorA-GFP (RR) was severely inhibited by CCCP (carbonyl cyanide 3-chlorophenylhydrazone), a protonophore, even if the reaction mixture contains DTT that inactivates CCCP, indicating that the translocation is dependent on PMF (right). Furthermore, omitting MPIase, TatABC, or F_0F_1-ATPase resulted in a loss of translocation activity (left). These results indicate that TatABC, MPIase, and PMF are necessary and sufficient for TAT translocation.

MPIase serves as the TAT signal receptor

Although the participation of MPIase in the TAT pathway has been demonstrated both in vivo and in vitro, the mechanisms by which MPIase contributes to TAT translocation remain unclear. Our previous study showed that the glycan chain and the pyrophosphate residue of MPIase captures the substrate membrane protein on the membrane surface before membrane insertion (***Fujikawa et al., 2023***; ***Nishikawa et al., 2022***). Although the TatBC complex has been shown to act as the TAT signal sequence receptor (***Cline and Mori, 2001***; ***Tarry et al., 2009***), we hypothesized that MPIase could also be involved in the targeting of the TAT substrate proteins to the membrane. Thus, we examined whether or not MPIase is involved in the membrane localization of TorA-GFP. Cells expressing TorA-GFP were fractionated into soluble (cytosol plus periplasm) and membrane fractions. Then, we measured the GFP fluorescence. We confirmed that the cell debris and microaggregates could be removed by low-speed centrifugation before membrane sedimentation (see ***Figure 1—figure supplement 2***). When we induced MPIase in KS23 cells by adding arabinose, ~30% of the fluorescence was recovered in the membrane fraction (***Figure 4A***, 'RR, +MPIase'), similarly to the 'EK413' case. Note that the MPIase level was insufficient under these conditions, resulting in very low translocation efficiency (see ***Figure 1B***). Conversely, when MPIase was depleted, only <10% of the fluorescence was recovered in the membrane fraction (***Figure 4A***, 'RR, ΔMPIase'). Similar results were obtained using TorA-GFP with a mutated signal sequence (KK; ***Figure 4A***). These results strongly suggest that MPIase serves as a receptor for the TAT signal, but that MPIase does not discriminate the functional signal. Similar to

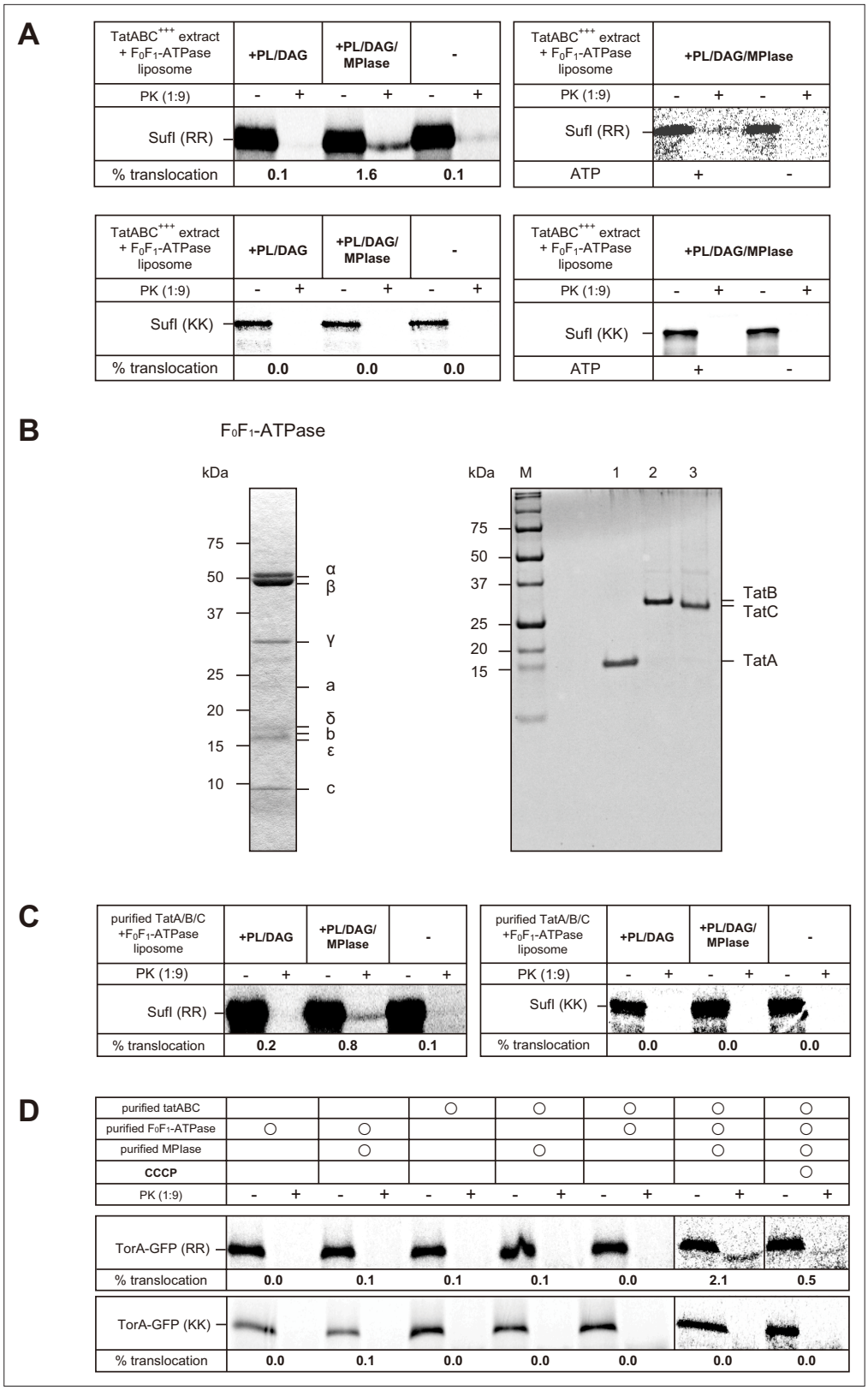


Figure 3. Reconstitution of the TAT system. (**A**) Membrane fusion of TatABC proteoliposomes with MPIase liposomes enabled the detection of the SufI translocation. INV, prepared from BL21/pT7-TatABC, were solubilized with OG, and then mixed with purified F_0F_1-ATPase. The proteoliposomes were then formed by removing the detergent. PL/DAG liposomes or PL/DAG/MPIase liposomes were fused to the reconstituted proteoliposomes.

Figure 3 continued on next page

Figure 3 continued

SufI translocation was performed co-translationally (left) or post-translationally (right) in the presence of these proteoliposomes. SufI(RR) (top left) or SufI(KK) (bottom left) was used as the substrate. One-ninth of the reaction mixture was analyzed as the translation standard (-) for the co-translational reactions. For the post-translational reactions, ATP was added as indicated. Translocation activities are shown at the bottom of the left panels. (**B**) Purification of F_0F_1-ATPase and the TAT components. F_0F_1-ATPase from a thermophilic Bacillus PS3 (left), and *E. coli* TatA-His (lane 1), TatB-His (lane 2), and TatC-His (lane 3) (right) were subjected to SDS-PAGE, followed by Coomassie Brilliant Blue staining. (**C, D**) Complete reconstitution of the TAT system using the purified components. (**C**) Purified TatA, TatB, and TatC (in a 1:1:1 ratio) and F_0F_1-ATPase were mixed with phospholipids. Then, detergent was removed to form proteoliposomes. The reconstituted proteoliposomes were then fused with PL/DAG liposomes or PL/DAG/MPIase liposomes. Translocation activity was assayed with SufI(RR) (left) or SufI(KK) (right). (**D**) Proteoliposomes were reconstituted with the indicated components, followed by TorA-GFP translocation. The TatA:TatB:TatC ratio was 10:1:1. CCCP (20 μM), a protonophore, was added to the sample on the left. TorA-GFP(RR) (top) or TorA-GFP(KK) (bottom) was used as the substrate. Translocation activities are shown at the bottom of each gel. Errors denote ± SD (N=3).

The online version of this article includes the following source data and figure supplement(s) for figure 3:

Source data 1. PDF file containing original autoradiographs for ***Figure 2***, indicating the relevant bands and treatments.

Source data 2. Original files for translocation analysis displayed in ***Figure 3***.

Figure supplement 1. In vivo complementation of the SDS-sensitive growth by His-tagged Tat components.

the '+MPIase' and 'EK413' cases, ~30% of the fluorescence was recovered in the membrane fraction when the *tatC* knockout mutant was used (***Figure 4A***, 'ΔTatC'). These results suggest that MPIase recognizes the TAT signal before TatC does. When GFP without the TAT signal was expressed, >90% of fluorescence was recovered in the supernatant fraction, regardless of MPIase levels and TatABC overproduction (***Figure 4—figure supplement 1***), indicating that the membrane localization depends solely on the TorA signal.

The MPIase-dependent membrane targeting was also observed using fluorescent microscopy (***Figure 4B***). When MPIase was induced by adding arabinose, an envelope-shaped fluorescence signal was detected, regardless of whether it was wild-type or mutant (***Figure 4B***, left), indicating that TorA-GFP (RR) and TorA-GFP (KK) were both targeted to membranes. Conversely, under the MPIase-depleted conditions, whole-cell fluorescence was detected (***Figure 4B***, right), indicating that both TorA-GFP (RR) and TorA-GFP (KK) located in the cytosol.

MPIase-dependent targeting was confirmed in vitro (***Figure 4C***, top). When the purified TorA-GFP (***Figure 4—figure supplement 2***) was mixed with wild-type INV (***Figure 4C***, 'EK413'), TatABC-overproducing INV (***Figure 4C***, 'TatABC^{+++}'), and TatC-deficient INV (***Figure 4C***, 'ΔTatC'), in all of which contain MPIase, fluorescent dots were observed, indicating that TorA-GFP directly interacts with these INV. The number of dots increased with TatABC overproduction, which is consistent with MPIase upregulation induced by TatABC overproduction. In contrast, no such fluorescent dots were observed in the presence of MPIase-depleted INV (***Figure 4C***, 'ΔMPIase'), confirming the MPIase-dependent targeting of TorA-GFP. The presence of similar amounts of membrane vesicles was visualized by adding fluorescent phospholipids, NBD-PE (***Figure 4C***, bottom).

Discussion

In this study, we demonstrated that glycolipid MPIase is essential for the TAT system. All of the in vivo, in vitro, and reconstitution studies supported this conclusion. Therefore, the previous unsuccessful attempts at TAT reconstitution were likely due to an insufficient amount of MPIase in TatABC proteoliposomes. Even when using solubilized membranes containing TatABC and MPIase to prepare proteoliposomes, MPIase recovery would be too low to detect the TAT activity.

MPIase is a glycolipid that catalyzes the membrane insertion of proteins with a single TM (***Nishiyama et al., 2010***; ***Endo et al., 2022***) as well as those with multiple TM domains (***Nishikawa et al., 2017***; ***Nishiyama et al., 2006***; ***Sasaki et al., 2019***). Therefore, depleting MPIase should impair the membrane insertion of all the TAT components, TatA, TatB, and TatC, leading to the failure of TAT translocation. However, in our experimental system, TatABC was still present after MPIase depletion

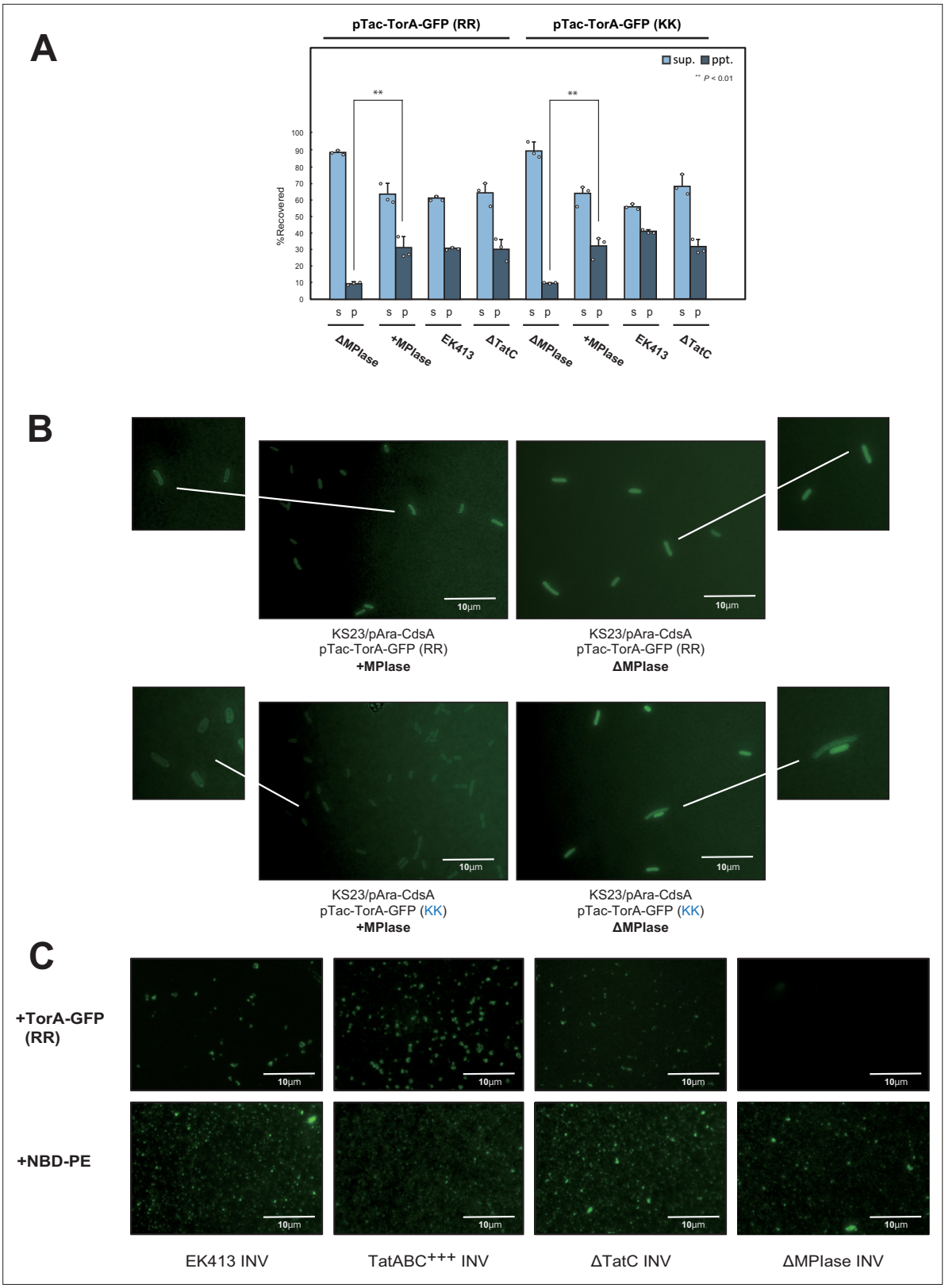


Figure 4. MPIase is a membrane receptor for TAT substrates. (**A,B**) TorA-GFP is targeted to the membrane in an MPIase-dependent manner. TorA-GFP(RR) (A; left half) or TorA-GFP(KK) (A; right half) was expressed in the specified strains. The cells were then disrupted to obtain the supernatant (sup; cytosol and periplasm) and the precipitate (ppt; membranes) fractions. The fluorescence intensity of each fraction was measured. The ratio to the whole cell was determined and shown as percentages. The means and standard deviations were calculated from at least three independent experiments.

Figure 4 continued on next page

Figure 4 continued

, p<0.01. In (B**), the indicated strains were cultivated, TorA-GFP was induced, and then it was observed by fluorescence microscopy. The scale bars represent 10 μm. Part of each picture was magnified on each side. Scale bars represent 10 μm. (**C**) TorA-GFP interacts with INV expressing MPIase. Purified TorA-GFP was mixed with the indicated INV, followed by fluorescence detection (top). As a control, each INV was mixed with NBD-PE, a fluorescent phospholipid, and observed (bottom). Scale bars represent 10 μm.

The online version of this article includes the following source data and figure supplement(s) for figure 4:

Source data 1. Excel files including the raw data for ***Figure 4A***, ***Figure 4—figure supplement 1***.

Figure supplement 1. GFP without the TAT signal is not targeted to the membrane.

Figure supplement 2. Purification of TorA-GFP.

Figure supplement 2—source data 1. PDF file containing original Coomassie Brilliant Blue-stained gel for ***Figure 4—figure supplement 2***, indicating the relevant bands and treatments.

Figure supplement 2—source data 2. Original files for the gel displayed in ***Figure 4—figure supplement 2***.

(see ***Figure 2C***), which supports the direct involvement of MPIase in the TAT translocation. Previous studies have reported that the Sec translocation slows down but does not stop completely when MPIase is depleted (***Sawasato et al., 2019a***), suggesting that the Sec machinery, including SecYEG, remains present during the initial stages of MPIase depletion, as demonstrated in this study. The results of the reconstitution study, in which TatABC was reconstituted in proteoliposome membranes, rule out the indirect involvement of MPIase in TAT translocation. In this system, the TAT translocation occurred in TatABC-, PMF-, and MPIase-dependent manners.

How is then MPIase involved in the TAT system? Since MPIase has been identified as a factor that catalyzes membrane protein integration (***Nishiyama et al., 2012***; ***Nishiyama et al., 2010***), it is possible that MPIase drives the insertion of the TAT signal sequences into membranes, thereby initiating the translocation reaction (***Figure 5***, (i)). Depleting MPIase caused TorA-GFP to accumulate in the cytosol. Thus, MPIase serves as a receptor for TAT precursors, and the TAT signal sequences are inserted into membranes. In this process, both hydrophobic interaction between the *h*-region and the acetyl residues of the MPIase glycan, and electrostatic interaction between the positive charges of the *n*-region and the pyrophosphate residue of MPIase would be involved, as observed in the interaction between substrate membrane proteins and MPIase (***Mori et al., 2022***). Then, they are transferred to TatC (ii), where the functional TAT signal is verified (iii). In addition to its roles as a membrane receptor and an insertase for the TAT signals, MPIase may facilitate structural changes in TatABC, allowing the complex to form the translocon dedicated to the substrate protein (iv). The TAT substrate is then translocated through the translocon, and the mature protein is released into the periplasm upon

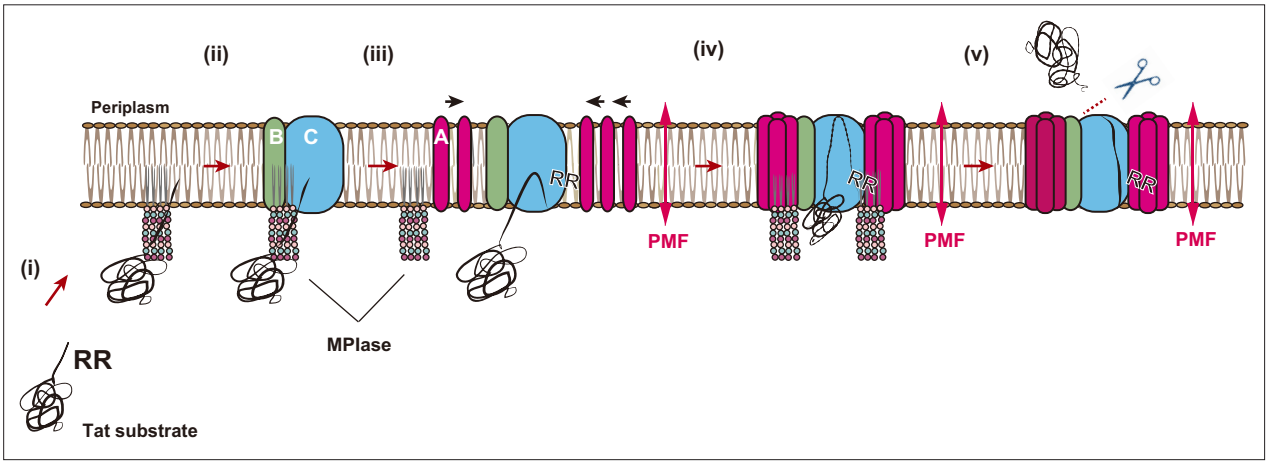


Figure 5. Working model of mechanisms underlying MPIase-dependent TAT translocation. MPIase recognizes the signal sequence of the TAT substrates and inserts them into the membrane. The TatBC complex on the membrane then determines whether the signal sequence of the membrane-inserted TAT substrate is valid. The TatABC translocon then forms a pore the same size as the substrate. This allows the substrate protein to be translocated across the membrane. Finally, Lep cleaves the signal sequence, and the mature protein is released into the periplasm. See the text for details.

Lep-mediated cleavage of the signal sequence (**Yahr and Wickner, 2001**; **Lüke et al., 2009**) (v). These processes require PMF, as previously reported (**Majdalani and Ippen-Ihler, 1996**). Thus, MPIase may be involved not only in the membrane targeting of TAT substrates but also in forming the TatABC translocon for each substrate. Membrane lipids PE may be important for these processes since PE is essential for TAT translocation **Rathmann et al., 2017**. In the reconstitution studies, the absence of DAG in (proteo)liposomes allowed for the spontaneous insertion of membrane proteins and signal sequences (**Nishiyama et al., 2006**; **Kawashima et al., 2008**). Therefore, the failure of the TAT reconstitution strongly suggests that MPIase has functions beyond serving as a membrane receptor and an insertase for TAT translocation. Given that MPIase induces dynamic structural changes in the SecYEG translocon (**Moser et al., 2013**; **Nishiyama et al., 1996**), it is likely that MPIase also modifies the structure of TatABC to form a tailor-made translocon. This possibility is consistent with the observations showing that TatABC overproduction induces MPIase upregulation and that MPIase co-precipitates with TatABC.

It is well known that the lipid environment of the membranes significantly affects the efficiency of TAT translocation. First, acidic phospholipids are important for TAT translocation because TAT signals interact with the acidic phospholipids (**Shanmugham et al., 2006**). MPIase has a pyrophosphate residue and would therefore contribute to this interaction in a similar way. At the same time, the hydrophobic domain of the TAT signals is solubilized by the glycan chain, as occurs with membrane proteins (**Mori et al., 2022**). Conversely, a decrease in PE (i.e. an increase in acidic phospholipids, PG, and CL) decreases efficiency (**Mikhaleva et al., 1999**; **Sikdar and Doerrler, 2010**), presumably due to overly strong interactions between the TAT signals and the acidic phospholipids. Alternatively, PE may be important for TAT translocation since it stabilizes several membrane proteins (**Bogdanov and Dowhan, 1998**). Thus, PE may be involved in the expression of the TatABC function. In the thylakoid system, the reduced unsaturation in membrane lipids results in a 50% decrease in the efficiency of TAT translocation (**Ma and Browse, 2006**), suggesting that membrane fluidity is also important for TAT translocation. We have demonstrated that MPIase increases the membrane fluidity through the flexible movement of its long sugar chain (**Nomura et al., 2019**). This property would benefit TAT translocation.

MPIase is upregulated in the cold. During this process, both *cdsA* and *ynbB* are induced at the transcriptional level. In the case of *cdsA* induction, two cold-inducible promoters located upstream of the *cdsA* gene are responsible (**Sawasato et al., 2019b**). MucA, a small peptide that overlaps with *cdsA*, enhances MPIase synthesis by CdsA (**Hikage et al., 2024**). When MPIase is upregulated by TatABC overproduction (see **Figure 2D**), *cdsA* and/or *ynbB* are also induced, as evidenced by the diminished increase in the MPIase level in *cdsA*/*ynbB* knockouts even when CdsA expression is complemented from the *araBAD* promoter on a plasmid. In this case, the *cdsA* promoters other than identified cold-inducible ones would be responsible, together with MucA. Alternatively, other mechanisms could operate to upregulate MPIase.

We found that the TAT translocation could be reconstituted with TatABC and MPIase alone when PMF was imposed, indicating that these factors are sufficient for TAT translocation. Although the activity was comparable to that of INV and proteoliposomes with the crude extract, it was still low. Therefore, these results suggest the presence of factor(s) involved in TAT translocation that stimulate the reaction, as the soluble factors that solubilize the TAT substrates and target them to membranes remain unidentified.

The TAT system is widely used as a carrier system for secreting foreign proteins into the medium (**Kikuchi et al., 2006**; **Kikuchi et al., 2009**; **Umakoshi et al., 2011**). Now that we know that MPIase is involved in the TAT system, it will be easier to engineer the TAT system by modulating the MPIase activity to increase the level of secreted proteins.

The TAT system was first identified in the thylakoid membranes of chloroplasts as a ΔpH-dependent pathway (**Mould and Robinson, 1991**; **Cline et al., 1992**). The components of the TAT system in chloroplasts are highly homologous to TatABC in *E. coli* (**Cline and Mori, 2001**; **Mori and Cline, 2002**), and the translocation reaction is also driven by PMF (**Mould and Robinson, 1991**). Thus, the mechanisms underlying the TAT systems in *E. coli* and chloroplasts likely have similar underlying mechanisms, strongly suggesting the presence of an MPIase homologue in chloroplasts. This similarity could facilitate the identification of an MPIase homologue in chloroplasts.

Materials and methods

Materials

The strains, plasmids, and oligonucleotides used in this study are listed in ***Supplementary file 1A, B and C***, respectively. INV were prepared as described ***Alami et al., 2002***. The plasmid pCspB-TorAss-GFP encoding TorA-GFP was obtained from Dr. Y. Kikuchi (Ajinomoto Co., Inc). Bio Beads SM-2 were purchased from Bio-Rad. [^{35}S] EXPRE^{35}S^{35}S Protein Labeling Mix, a mixture of [^{35}S] methionine and [^{35}S] cysteine (~37 TBq/mmol), was obtained from Revvity. Proteinase K (PK) was purchased from Roche Diagnostics. The cell-free protein synthesis kit '*E. coli* S30 Extract System for Circular DNA' was purchased from Promega Corporation. The *E. coli* polar lipid extract (phospholipids), 18:1 NBD-PE, and dioleoylglycerol were obtained from Avanti Polar Lipids, Inc *n*-Octyl-β-D-glucopyranoside (OG) and *n*-dodecyl-β-D-maltopyranoside (DDM) were obtained from Dojindo Laboratories. IPTG was from Wako Pure Chemicals Industries, Ltd. TLC plates were from Merck. MPIase was purified from MC4100, as described (***Nishiyama et al., 2012***; ***Nishiyama et al., 2010***). TorA-GFP, TatA, TatB, TatC, and the TatABC complex were purified from DH5α/pTac-TorA-GFP-His, DH5α/pTac-TatA-His, DH5α/pTac-TatB-His, DH5α/pTac-TatC-His, BL21/pT7-Pm-F_0b-His, and BL21/pT7-TatABC-His, respectively. These proteins were induced with 1 mM IPTG, followed by INV preparation, solubilization, and purification through the 6 x His-tag attached to C-termini on Talon columns. The conditions for INV solubilization and Talon column chromatography were carried out as described (***Sasaki et al., 2019***). Purification of F_0F_1-ATPase from a thermophilic bacterium PS3 was performed as described (***Suzuki et al., 2002***). Antibodies against β-lactamase and GFP were commercially obtained from 5 Prime -->3 Prime, Inc and Medical & Biological Laboratories Co., Ltd., respectively. Anti-SecB (***Sawasato et al., 2019a***), anti-RpmJ-His (***Ikegami et al., 2005***), anti-TatA (***Rose et al., 2013***), and anti-MPIase (***Nishiyama et al., 2012***) antibodies, raised in rabbits, were also used.

Depletion of MPIase

Strains KS23/pAra-CdsA and KS46/pAra-CdsA were cultivated overnight at 37 °C in LB medium containing 0.002% arabinose. After the cells were washed five times with fresh LB medium, they were inoculated into LB medium supplemented or not with 0.2% arabinose at a dilution of 1/1000 and then shaken at 37 °C. To express the TAT substrates, IPTG (1 mM) was added after the cell culture was grown to $OD_{600\ nm}$ ~0.5 and cultivated for another 1 hr. An aliquot (500 µL) of each sample was treated with TCA to a final concentration of 5%. The TCA precipitate was recovered by centrifugation (10,000 × *g*, 4 °C, 5 min), followed by washing with acetone. MPIase depletion was then confirmed by SDS-PAGE/immunoblotting, as described (***Sawasato et al., 2019a***).

Pulse-chase experiments

Cell cultures grown in LB medium to $OD_{600\ nm}$ ~0.5 were harvested and resuspended in M9 minimal medium containing 18 amino acids (0.1 mM each) except for methionine and cysteine, and 0.1% yeast extract. After incubating for an additional 1 hr at 37 °C, the substrate proteins were labeled with [^{35}S] methionine/cysteine (~10 MBq/mL) for 30 s. Labeling was terminated by adding non-radioactive methionine and cysteine to a final concentration of 12 mM. At the specified chase time, an aliquot (500 µL) of the culture was withdrawn, and TCA was added to a final concentration of 10%. The TCA precipitates were washed successively with acetone and diethyl ether, and then suspended in 50 µL of 50 mM Tris-HCl (pH 7.5), 1% SDS, 1 mM EDTA (pH 8.0), and boiled for 3 min. The samples were then diluted with 1 mL of 50 mM HEPES-KOH (pH 7.5), 150 mM NaCl, 1% Triton X-100, 1 mM EDTA (pH 8.0), 1 mM phenylmethylsulfonyl fluoride, and were centrifuged at 16,000 × *g* for 5 min. Then, 10 µL of TALON resin was added to the supernatant, and the mixture was stirred at 4 °C for 1 hr. After centrifugation (3,000 x g, 4 °C, 30 s), the TALON resin was washed successively with 500 µL of 50 mM Tris-HCl (pH 7.5), 150 mM NaCl, 1% Triton X-100. The washed resin was suspended in 20 µL of the sample buffer for SDS-PAGE. Radioactive bands, analyzed by SDS-PAGE, were detected by autoradiography using a phosphorimager (GE Healthcare), and quantified using ImageQuant (GE Healthcare).

Preparation and fractionation of spheroplasts

After the cells were grown in LB medium to $OD_{600\ nm}$ ~0.5, 1 mM IPTG was added to induce the TAT substrates. The cells were harvested at 2400 × *g* for 5 min and washed with 5 mL of 0.75 M sucrose, 10 mM Tris-HCl (pH 7.5). They were then suspended in 1 mL of 0.75 M sucrose, 10 mM Tris-HCl (pH

7.5), and 20 μg/mL lysozyme solution and incubated on ice for 5 min. They were converted into spheroplasts by adding 1.5 mM EDTA (pH 8.0) at equal intervals over 10 min, bringing the total volume to 2 mL. An aliquot of the spheroplast suspension (1 mL) was centrifuged (15,000 × *g*, 4 °C, 1 min) to sediment spheroplasts. The spheroplasts were suspended in 500 μL water and treated with 10% TCA, followed by incubation on ice for 10 min to precipitate proteins. The periplasmic fraction, obtained by sedimentation of the spheroplasts, was treated similarly. The proteins were then recovered by centrifugation (10,000 × *g*, 4 °C, 5 min), washed with acetone, and subjected to SDS-PAGE/immunoblotting, as previously described (***Nishikawa et al., 2020***).

Fluorescence microscopy

E. coli strains were grown in LB medium to $OD_{600\ nm}$ ~0.5, followed by the addition of 1 mM IPTG to induce TorA-GFP. The cells were fixed on glass slides coated with 1% agarose, as described (***Rose et al., 2013***). The cells were observed using a fluorescence microscope (Olympus BX53, combined with a U-FGFP filter). Images were captured with a 3CCD digital camera (Olympus DP74). The digital images were then processed and analyzed using the cell image analysis software, cellSens Standard (Olympus).

Assaying of the protein translocation in vitro

The TAT substrates were synthesized in vitro using the *E. coli* T7 S30 extract system. For the co-translational translocation assay, the following were added to a 20 μL reaction mixture: [^{35}S] methionine and cysteine (~10 MBq/mL), plasmids encoding the substrate protein under the T7 promoter, and INV or proteoliposomes. The synthesis/translocation of the RI-labeled substrates was performed at 37 °C for 1 hr. When INV was used, it was added to the reaction mixture 5 min after the reaction started. For the post-translational translocation assay, the RI-labeled substrates (3 μL), synthesized in the absence of INV or proteoliposomes at 30 °C for 30 min, were added to a translocation mixture containing 50 mM HEPES-KOH (pH 7.5), INV or proteoliposomes, 1 mM $MgSO_4$, 5 mM creatine phosphate, 10 μg/mL creatine kinase, and 1 mM ATP. After incubating the mixture at 37 °C for 45 min, it was divided into two portions. One portion was treated with 5% TCA to precipitate the substrate proteins. The other portion was mixed with an equal volume of PK (1 mg/mL) and incubated at 25 °C for 20 min. After adding 5% TCA, the samples were incubated at 56 °C for 5 min to inactivate PK. Then, the proteins were recovered by centrifugation (10,000 × *g*, 4 °C, 5 min). Radioactive materials were detected and quantified as described above.

TALON affinity chromatography

INV (4 mg protein) was solubilized using 1% DDM, 20% glycerol, 50 mM HEPES-KOH (pH 7.5). The solubilized membranes were recovered by centrifugation (170,000 × *g*, 4 °C, 30 min). Samples were applied to a TALON column (0.5 mL). After washing the column with 20 mL of 0.02% DDM, 10% glycerol, and 50 mM HEPES-KOH (pH 7.5), the column-bound materials were eluted with the same buffer containing 150 mM imidazole. The eluted fraction was analyzed by TLC using a solvent system C (chloroform/ethanol/water: 3/7/4) for development. Then, MPIase was detected using anti-MPIase antibody, as described (***Endo et al., 2022***).

Reconstitution of proteoliposomes

Phospholipids (13 mg) were resuspended in buffer A (50 mM HEPES-KOH (pH 7.5), 1 mM dithiothreitol) at 20 mg/mL, followed by bath sonication to form liposomes. The liposomes were solubilized in 5% [w/v] OG and incubated on ice for 15 min. Then, 200 mg of Bio Beads SM-2 were added, and the mixture was gently stirred at 4 °C for 30 min. Purified TatA (100 μg or 1000 μg), TatB (100 μg), TatC (100 μg), and F_0F_1-ATPase (1 μM) were added to the solution. The solution was gently mixed at 4 °C for at least 3 hr. The Bio Beads SM-2 were then removed, and the proteoliposomes were recovered by centrifugation (170,000 × *g*, 4 °C, 1 hr). DAG- and DAG/MPIase-containing liposomes were prepared, as described (***Nishikawa et al., 2020***). TatABC/F_0F_1-ATPase proteoliposomes and PL/DAG liposomes or PL/DAG/MPIase liposomes were typically mixed at a ratio of 4:1, followed by three cycles of freezing, thawing, and sonicating to allow liposome fusion, as described (***Nishiyama et al., 1996***). As a result of liposome fusion, proteoliposomes contain DAG and MPIase at 5% each

to phospholipids. The mixture was then passed through a mini-extruder (Avanti Polar Lipids, Inc) with a 0.4 μm pore size filter to obtain uniformly sized liposomes, as described (***Kawashima et al., 2008***).

Subcellular fractionation

After the cells were grown in LB medium to $OD_{600\ nm}$ ~0.5, 1 mM IPTG was added to induce the TAT substrates. The harvested cells were suspended in 50 mM HEPES-KOH (pH 7.5), 10% glycerol, 1 mM dithiothreitol, 1 mM phenylmethylsulfonyl fluoride, protease inhibitor cocktail (Roche), and then disrupted using a French press. Then, the cells were incubated with 2 mM $MgSO_4$, DNase I (1 mg/mL) on ice for 15 min, followed by the addition of 2 mM EDTA (pH 8.0) and incubation on ice for an additional 15 min. The disrupted and undisrupted cells were separated by centrifugation (15,000 × *g*, 4 °C, 10 min), and then they were fractionated into soluble (cytosol and periplasm) and insoluble (membrane) fractions by centrifugation (150,000 × *g*, 4 °C, 1 hr). TorA-GFP was detected by monitoring GFP fluorescence. Samples were added to 2 mL of 50 mM HEPES-KOH (pH 7.5), and the fluorescence intensity was measured at an excitation of 395 nm and an emission of 509 nm using an FP-8200 fluorescence spectrometer (JASCO).

Statistical analysis

Statistical significance was determined using a Student's t-test. The p values of less than 0.05 were considered significant.

Other methods

SDS-PAGE was performed using 12.5% acrylamide/0.27% *N*,*N*'-bis (methyleneacrylamide; ***Hussain et al., 1980***) for TatA, TatB, TatC, SecB, β-lactamase, and MPIase. 15.0% acrylamide/0.33% *N*,*N*'-bis (methyleneacrylamide; ***Laemmli, 1970***) was used to analyze SufI and TorA-GFP, while 8% acrylamide/0.17% *N*,*N*'-bis (methyleneacrylamide) was used for TorA. Bands on the immunoblots were quantified using a CS analyzer (ATTO). Protein quantification after INV preparation was performed using bovine serum albumin as a standard, as described (***Lowry et al., 1951***). Detection of MPIase and other proteins by immunoblotting was performed as described (***Sawasato et al., 2019a***; ***Ikegami et al., 2005***).

Acknowledgements

We thank Prof. Matthias Müller for the fruitful discussions and antibodies; Dr. Yoshimi Kikuchi for the discussions and plasmids encoding TorA-GFP; and Ms. Hiromi Saito, Mari Saikudo, and Miki Sawaguchi for the MPIase purification. We also thank NBRP (NIG, Japan): *E. coli* for the Keio clones. Experiments involving radioisotopes were carried out in the RI Laboratory at Iwate University. Research reported in this publication was supported by the Noguchi Shitagau Research Grant to HN and JSPS KAKENHI grants to HN and KN (grant numbers: 18J21847 to HN; 22H02567, 22K19262, 22H05392, 23H04536, and 24H01107 to KN).

Additional information

Funding

Funder	Grant reference number	Author
Japan Society for the Promotion of Science	18J21847	Hanako Nishikawa
Japan Society for the Promotion of Science	22H02567	Ken-ichi Nishiyama
Japan Society for the Promotion of Science	22K19262	Ken-ichi Nishiyama
Japan Society for the Promotion of Science	22H05392	Ken-ichi Nishiyama

Funder	Grant reference number	Author
Japan Society for the Promotion of Science	23H04536	Ken-ichi Nishiyama
Japan Society for the Promotion of Science	24H01107	Ken-ichi Nishiyama
Noguchi Shitagau Research Grant		Hanako Nishikawa

The funders had no role in study design, data collection and interpretation, or the decision to submit the work for publication.

Author contributions

Hanako Nishikawa, Conceptualization, Data curation, Supervision, Funding acquisition, Validation, Investigation, Writing – original draft, Writing – review and editing; Nachi Yamamoto, Data curation, Investigation, Visualization; Hayate Kunezaki, Yui Shirogane, Data curation, Investigation; Kotoka Kanno, Conceptualization, Data curation, Investigation; Katsuhiro Sawasato, Conceptualization, Data curation, Supervision, Investigation; Miwa Yamada, Conceptualization, Resources; Ken-ichi Nishiyama, Conceptualization, Supervision, Funding acquisition, Writing – original draft, Project administration, Writing – review and editing

Author ORCIDs

Hanako Nishikawa https://orcid.org/0009-0002-9443-6376
Katsuhiro Sawasato https://orcid.org/0000-0001-9965-970X
Miwa Yamada https://orcid.org/0000-0003-1038-0505
Ken-ichi Nishiyama https://orcid.org/0000-0003-0478-4482

Peer review material

Version of Record:
Reviewer #2 (Public review): https://doi.org/10.7554/eLife.112170.4.sa1
Author response https://doi.org/10.7554/eLife.112170.4.sa2

Reviewed preprint v3
Reviewer #2 (Public review): https://doi.org/10.7554/eLife.112170.3.sa1
Author response: https://doi.org/10.7554/eLife.112170.3.sa0
eLife Assessment https://doi.org/10.7554/eLife.112170.3.sa2

Reviewed preprint v2
Reviewer #1 (Public review): https://doi.org/10.7554/eLife.112170.2.sa2
Reviewer #2 (Public review): https://doi.org/10.7554/eLife.112170.2.sa1
Author response: https://doi.org/10.7554/eLife.112170.2.sa0
eLife Assessment https://doi.org/10.7554/eLife.112170.2.sa3

Reviewed preprint v1
Reviewer #1 (Public review): https://doi.org/10.7554/eLife.112170.1.sa1
Reviewer #2 (Public review): https://doi.org/10.7554/eLife.112170.1.sa0
eLife Assessment https://doi.org/10.7554/eLife.112170.1.sa2

Additional files

Supplementary files

Supplementary file 1. Bacterial strains (Table A), plasmids (Table B), and oligonucleotides (Table C) used in this study.

MDAR checklist

Data availability

All data generated or analyzed during this study are included in the manuscript, supporting files and source data files.

References

Alami M, Trescher D, Wu LF, Müller M. 2002. Separate analysis of twin-arginine translocation (Tat)-specific membrane binding and translocation in *Escherichia coli*. *The Journal of Biological Chemistry* **277**:20499–20503. DOI: https://doi.org/10.1074/jbc.M201711200, PMID: 11923313

Alami M, Lüke I, Deitermann S, Eisner G, Koch HG, Brunner J, Müller M. 2003. Differential interactions between a twin-arginine signal peptide and its translocase in *Escherichia coli*. *Molecular Cell* **12**:937–946. DOI: https://doi.org/10.1016/s1097-2765(03)00398-8, PMID: 14580344

Alcock F, Baker MAB, Greene NP, Palmer T, Wallace MI, Berks BC. 2013. Live cell imaging shows reversible assembly of the TatA component of the twin-arginine protein transport system. *PNAS* **110**:E3650–E3659. DOI: https://doi.org/10.1073/pnas.1306738110, PMID: 24003141

Bageshwar UK, Musser SM. 2007. Two electrical potential-dependent steps are required for transport by the *Escherichia coli* Tat machinery. *The Journal of Cell Biology* **179**:87–99. DOI: https://doi.org/10.1083/jcb.200702082, PMID: 17908913

Beck D, Vasisht N, Baglieri J, Monteferrante CG, van Dijl JM, Robinson C, Smith CJ. 2013. Ultrastructural characterisation of *Bacillus subtilis* TatA complexes suggests they are too small to form homooligomeric translocation pores. *Biochimica et Biophysica Acta* **1833**:1811–1819. DOI: https://doi.org/10.1016/j.bbamcr.2013.03.028, PMID: 23567937

Berks BC. 1996. A common export pathway for proteins binding complex redox cofactors? *Molecular Microbiology* **22**:393–404. DOI: https://doi.org/10.1046/j.1365-2958.1996.00114.x, PMID: 8939424

Berks BC. 2015. The twin-arginine protein translocation pathway. *Annual Review of Biochemistry* **84**:843–864. DOI: https://doi.org/10.1146/annurev-biochem-060614-034251, PMID: 25494301

Blaudeck N, Kreutzenbeck P, Freudl R, Sprenger GA. 2003. Genetic analysis of pathway specificity during posttranslational protein translocation across the *Escherichia coli* plasma membrane. *Journal of Bacteriology* **185**:2811–2819. DOI: https://doi.org/10.1128/JB.185.9.2811-2819.2003, PMID: 12700260

Bogdanov M, Dowhan W. 1998. Phospholipid-assisted protein folding: phosphatidylethanolamine is required at a late step of the conformational maturation of the polytopic membrane protein lactose permease. *The EMBO Journal* **17**:5255–5264. DOI: https://doi.org/10.1093/emboj/17.18.5255, PMID: 9736605

Bogsch E, Brink S, Robinson C. 1997. Pathway specificity for a delta pH-dependent precursor thylakoid lumen protein is governed by a "Sec-avoidance" motif in the transfer peptide and a "Sec-incompatible" mature protein. *The EMBO Journal* **16**:3851–3859. DOI: https://doi.org/10.1093/emboj/16.13.3851, PMID: 9233795

Bogsch EG, Sargent F, Stanley NR, Berks BC, Robinson C, Palmer T. 1998. An essential component of a novel bacterial protein export system with homologues in plastids and mitochondria. *The Journal of Biological Chemistry* **273**:18003–18006. DOI: https://doi.org/10.1074/jbc.273.29.18003, PMID: 9660752

Bolhuis A, Mathers JE, Thomas JD, Barrett CM, Robinson C. 2001. TatB and TatC form a functional and structural unit of the twin-arginine translocase from *Escherichia coli*. *The Journal of Biological Chemistry* **276**:20213–20219. DOI: https://doi.org/10.1074/jbc.M100682200, PMID: 11279240

Brüser T, Sanders C. 2003. An alternative model of the twin arginine translocation system. *Microbiological Research* **158**:7–17. DOI: https://doi.org/10.1078/0944-5013-00176, PMID: 12608575

Chaddock AM, Mant A, Karnauchov I, Brink S, Herrmann RG, Klösgen RB, Robinson C. 1995. A new type of signal peptide: central role of a twin-arginine motif in transfer signals for the delta pH-dependent thylakoidal protein translocase. *The EMBO Journal* **14**:2715–2722. DOI: https://doi.org/10.1002/j.1460-2075.1995.tb07272.x, PMID: 7796800

Cline K, Ettinger WF, Theg SM. 1992. Protein-specific energy requirements for protein transport across or into thylakoid membranes: Two lumenal proteins are transported in the absence of ATP. *The Journal of Biological Chemistry* **267**:2688–2696 PMID: 1733965.

Cline K, Mori H. 2001. Thylakoid DeltapH-dependent precursor proteins bind to a cpTatC-Hcf106 complex before Tha4-dependent transport. *The Journal of Cell Biology* **154**:719–729. DOI: https://doi.org/10.1083/jcb.200105149, PMID: 11502764

Cline K, McCaffery M. 2007. Evidence for a dynamic and transient pathway through the TAT protein transport machinery. *The EMBO Journal* **26**:3039–3049. DOI: https://doi.org/10.1038/sj.emboj.7601759, PMID: 17568769

Cristóbal S, de Gier JW, Nielsen H, von Heijne G. 1999. Competition between Sec- and TAT-dependent protein translocation in *Escherichia coli*. *The EMBO Journal* **18**:2982–2990. DOI: https://doi.org/10.1093/emboj/18.11.2982, PMID: 10357811

Dabney-Smith C, Mori H, Cline K. 2006. Oligomers of Tha4 organize at the thylakoid Tat translocase during protein transport. *The Journal of Biological Chemistry* **281**:5476–5483. DOI: https://doi.org/10.1074/jbc.M512453200, PMID: 16407186

Dabney-Smith C, Cline K. 2009. Clustering of C-terminal stromal domains of Tha4 homo-oligomers during translocation by the Tat protein transport system. *Molecular Biology of the Cell* **20**:2060–2069. DOI: https://doi.org/10.1091/mbc.e08-12-1189, PMID: 19193764

De Leeuw E, Porcelli I, Sargent F, Palmer T, Berks BC. 2001. Membrane interactions and self-association of the TatA and TatB components of the twin-arginine translocation pathway. *FEBS Letters* **506**:143–148. DOI: https://doi.org/10.1016/s0014-5793(01)02904-0, PMID: 11591389

de Leeuw E, Granjon T, Porcelli I, Alami M, Carr SB, Müller M, Sargent F, Palmer T, Berks BC. 2002. Oligomeric properties and signal peptide binding by *Escherichia coli* Tat protein transport complexes. *Journal of Molecular Biology* **322**:1135–1146. DOI: https://doi.org/10.1016/s0022-2836(02)00820-3, PMID: 12367533

Endo Y, Shimizu Y, Nishikawa H, Sawasato K, Nishiyama K-I. 2022. Interplay between MPIase, YidC, and PMF during Sec-independent insertion of membrane proteins. *Life Science Alliance* **5**:e202101162. DOI: https://doi.org/10.26508/lsa.202101162, PMID: 34642230

Fujikawa K, Han Y, Osawa T, Mori S, Nomura K, Muramoto M, Nishiyama K-I, Shimamoto K. 2023. Structural requirements of a glycolipid mpiase for membrane protein integration. *Chemistry* **29**:e202300437. DOI: https://doi.org/10.1002/chem.202300437, PMID: 36896742

Gohlke U, Pullan L, McDevitt CA, Porcelli I, de Leeuw E, Palmer T, Saibil HR, Berks BC. 2005. The TatA component of the twin-arginine protein transport system forms channel complexes of variable diameter. *PNAS* **102**:10482–10486. DOI: https://doi.org/10.1073/pnas.0503558102, PMID: 16027357

Hicks MG, de Leeuw E, Porcelli I, Buchanan G, Berks BC, Palmer T. 2003. The *Escherichia coli* twin-arginine translocase: conserved residues of TatA and TatB family components involved in protein transport. *FEBS Letters* **539**:61–67. DOI: https://doi.org/10.1016/s0014-5793(03)00198-4, PMID: 12650927

Hikage R, Tadika Y, Asanuma H, Han Y, Nishiyama K-I. 2024. MucA is a small peptide encoded by an overlapping sequence with cdsA that upregulates the biosynthesis of glycolipid MPIase in the cold. *Biochemical and Biophysical Research Communications* **721**:150148. DOI: https://doi.org/10.1016/j.bbrc.2024.150148, PMID: 38781662

Hussain M, Ichihara S, Mizushima S. 1980. Accumulation of glyceride-containing precursor of the outer membrane lipoprotein in the cytoplasmic membrane of *Escherichia coli* treated with globomycin. *The Journal of Biological Chemistry* **255**:3707–3712 PMID: 6988430.

Ikegami A, Nishiyama K, Matsuyama S, Tokuda H. 2005. Disruption of rpmJ encoding ribosomal protein L36 decreases the expression of secY upstream of the spc operon and inhibits protein translocation in *Escherichia coli*. *Bioscience, Biotechnology, and Biochemistry* **69**:1595–1602. DOI: https://doi.org/10.1271/bbb.69.1595, PMID: 16116291

Jack RL, Sargent F, Berks BC, Sawers G, Palmer T. 2001. Constitutive expression of *Escherichia coli* tat genes indicates an important role for the twin-arginine translocase during aerobic and anaerobic growth. *Journal of Bacteriology* **183**:1801–1804. DOI: https://doi.org/10.1128/JB.183.5.1801-1804.2001, PMID: 11160116

Kawashima Y, Miyazaki E, Müller M, Tokuda H, Nishiyama K. 2008. Diacylglycerol specifically blocks spontaneous integration of membrane proteins and allows detection of a factor-assisted integration. *The Journal of Biological Chemistry* **283**:24489–24496. DOI: https://doi.org/10.1074/jbc.M801812200, PMID: 18614537

Kikuchi Y, Date M, Itaya H, Matsui K, Wu LF. 2006. Functional analysis of the twin-arginine translocation pathway in Corynebacterium glutamicum ATCC 13869. *Applied and Environmental Microbiology* **72**:7183–7192. DOI: https://doi.org/10.1128/AEM.01528-06, PMID: 16997984

Kikuchi Y, Itaya H, Date M, Matsui K, Wu LF. 2009. TatABC overexpression improves Corynebacterium glutamicum Tat-dependent protein secretion. *Applied and Environmental Microbiology* **75**:603–607. DOI: https://doi.org/10.1128/AEM.01874-08, PMID: 19074606

Laemmli UK. 1970. Cleavage of structural proteins during the assembly of the head of bacteriophage T4. *Nature* **227**:680–685. DOI: https://doi.org/10.1038/227680a0, PMID: 5432063

Leake MC, Greene NP, Godun RM, Granjon T, Buchanan G, Chen S, Berry RM, Palmer T, Berks BC. 2008. Variable stoichiometry of the TatA component of the twin-arginine protein transport system observed by in vivo single-molecule imaging. *PNAS* **105**:15376–15381. DOI: https://doi.org/10.1073/pnas.0806338105, PMID: 18832162

Lowry OH, Rosebrough NJ, Farr AL, Randall RJ. 1951. Protein measurement with the Folin phenol reagent. *The Journal of Biological Chemistry* **193**:265–275 PMID: 14907713.

Lüke I, Handford JI, Palmer T, Sargent F. 2009. Proteolytic processing of *Escherichia coli* twin-arginine signal peptides by LepB. *Archives of Microbiology* **191**:919–925. DOI: https://doi.org/10.1007/s00203-009-0516-5, PMID: 19809807

Ma X, Browse J. 2006. Altered rates of protein transport in Arabidopsis mutants deficient in chloroplast membrane unsaturation. *Phytochemistry* **67**:1629–1636. DOI: https://doi.org/10.1016/j.phytochem.2006.04.008, PMID: 16759675

Majdalani N, Ippen-Ihler K. 1996. Membrane insertion of the F-pilin subunit is Sec independent but requires leader peptidase B and the proton motive force. *Journal of Bacteriology* **178**:3742–3747. DOI: https://doi.org/10.1128/jb.178.13.3742-3747.1996, PMID: 8682775

McDevitt CA, Buchanan G, Sargent F, Palmer T, Berks BC. 2006. Subunit composition and in vivo substrate-binding characteristics of *Escherichia coli* Tat protein complexes expressed at native levels. *The FEBS Journal* **273**:5656–5668. DOI: https://doi.org/10.1111/j.1742-4658.2006.05554.x, PMID: 17212781

Mehner-Breitfeld D, Ringel MT, Tichy DA, Endter LJ, Stroh KS, Lünsdorf H, Risselada HJ, Brüser T. 2022. TatA and TatB generate a hydrophobic mismatch important for the function and assembly of the Tat translocon in *Escherichia coli*. *The Journal of Biological Chemistry* **298**:102236. DOI: https://doi.org/10.1016/j.jbc.2022.102236, PMID: 35809643

Mikhaleva NI, Santini CL, Giordano G, Nesmeyanova MA, Wu LF. 1999. Requirement for phospholipids of the translocation of the trimethylamine N-oxide reductase through the Tat pathway in *Escherichia coli*. *FEBS Letters* **463**:331–335. DOI: https://doi.org/10.1016/s0014-5793(99)01661-0, PMID: 10606748

Mori H, Cline K. 2002. A twin arginine signal peptide and the pH gradient trigger reversible assembly of the thylakoid [Delta]pH/Tat translocase. *The Journal of Cell Biology* **157**:205–210. DOI: https://doi.org/10.1083/jcb.200202048, PMID: 11956224

Mori S, Nomura K, Fujikawa K, Osawa T, Shionyu M, Yoda T, Shirai T, Tsuda S, Yoshizawa-Kumagaye K, Masuda S, Nishio H, Yoshiya T, Suzuki S, Muramoto M, Nishiyama K-I, Shimamoto K. 2022. Intermolecular interactions between a membrane protein and a glycolipid essential for membrane protein integration. *ACS Chemical Biology* **17**:609–618. DOI: https://doi.org/10.1021/acschembio.1c00882, PMID: 35239308

Moser M, Nagamori S, Huber M, Tokuda H, Nishiyama K. 2013. Glycolipozyme MPIase is essential for topology inversion of SecG during preprotein translocation. *PNAS* **110**:9734–9739. DOI: https://doi.org/10.1073/pnas.1303160110, PMID: 23716687

Mould RM, Robinson C. 1991. A proton gradient is required for the transport of two lumenal oxygen-evolving proteins across the thylakoid membrane. *The Journal of Biological Chemistry* **266**:12189–12193 PMID: 1648086.

Nishikawa H, Sasaki M, Nishiyama K. 2017. Membrane insertion of F_0 c subunit of F_0F_1 ATPase depends on glycolipozyme MPIase and is stimulated by YidC. *Biochemical and Biophysical Research Communications* **487**:477–482. DOI: https://doi.org/10.1016/j.bbrc.2017.04.095

Nishikawa H, Sasaki M, Nishiyama KI. 2020. *In vitro* Assay for bacterial membrane protein integration into proteoliposomes. *Bio-Protocol* **10**:e3626. DOI: https://doi.org/10.21769/BioProtoc.3626, PMID: 33659299

Nishikawa H, Sawasato K, Mori S, Fujikawa K, Nomura K, Shimamoto K, Nishiyama KI. 2022. Interaction between glycolipid MPIase and proteinaceous factors during protein integration into the cytoplasmic membrane of *E. coli*. *Frontiers in Molecular Biosciences* **9**:986602. DOI: https://doi.org/10.3389/fmolb.2022.986602, PMID: 36060260

Nishiyama K, Suzuki T, Tokuda H. 1996. Inversion of the membrane topology of SecG coupled with SecA-dependent preprotein translocation. *Cell* **85**:71–81. DOI: https://doi.org/10.1016/s0092-8674(00)81083-1, PMID: 8620539

Nishiyama K, Ikegami A, Moser M, Schiltz E, Tokuda H, Müller M. 2006. A derivative of lipid A is involved in signal recognition particle/SecYEG-dependent and -independent membrane integrations. *The Journal of Biological Chemistry* **281**:35667–35676. DOI: https://doi.org/10.1074/jbc.M608228200, PMID: 17008318

Nishiyama K, Maeda M, Abe M, Kanamori T, Shimamoto K, Kusumoto S, Ueda T, Tokuda H. 2010. A novel complete reconstitution system for membrane integration of the simplest membrane protein. *Biochemical and Biophysical Research Communications* **394**:733–736. DOI: https://doi.org/10.1016/j.bbrc.2010.03.061, PMID: 20230783

Nishiyama K, Maeda M, Yanagisawa K, Nagase R, Komura H, Iwashita T, Yamagaki T, Kusumoto S, Tokuda H, Shimamoto K. 2012. MPIase is a glycolipozyme essential for membrane protein integration. *Nature Communications* **3**:1260. DOI: https://doi.org/10.1038/ncomms2267, PMID: 23232390

Nomura K, Yamaguchi T, Mori S, Fujikawa K, Nishiyama K-I, Shimanouchi T, Tanimoto Y, Morigaki K, Shimamoto K. 2019. Alteration of membrane physicochemical properties by two factors for membrane protein integration. *Biophysical Journal* **117**:99–110. DOI: https://doi.org/10.1016/j.bpj.2019.05.014, PMID: 31164197

Oates J, Barrett CML, Barnett JP, Byrne KG, Bolhuis A, Robinson C. 2005. The *Escherichia coli* twin-arginine translocation apparatus incorporates a distinct form of TatABC complex, spectrum of modular TatA complexes and minor TatAB complex. *Journal of Molecular Biology* **346**:295–305. DOI: https://doi.org/10.1016/j.jmb.2004.11.047, PMID: 15663945

Palmer T, Sargent F, Berks BC. 2005. Export of complex cofactor-containing proteins by the bacterial Tat pathway. *Trends in Microbiology* **13**:175–180. DOI: https://doi.org/10.1016/j.tim.2005.02.002, PMID: 15817387

Ramasamy S, Abrol R, Suloway CJM, Clemons WM. 2013. The glove-like structure of the conserved membrane protein TatC provides insight into signal sequence recognition in twin-arginine translocation. *Structure* **21**:777–788. DOI: https://doi.org/10.1016/j.str.2013.03.004, PMID: 23583035

Rathmann C, Schlösser AS, Schiller J, Bogdanov M, Brüser T. 2017. Tat transport in *Escherichia coli* requires zwitterionic phosphatidylethanolamine but no specific negatively charged phospholipid. *FEBS Letters* **591**:2848–2858. DOI: https://doi.org/10.1002/1873-3468.12794, PMID: 28815570

Richter S, Brüser T. 2005. Targeting of unfolded PhoA to the TAT translocon of *Escherichia coli*. *The Journal of Biological Chemistry* **280**:42723–42730. DOI: https://doi.org/10.1074/jbc.M509570200, PMID: 16263723

Rodriguez F, Rouse SL, Tait CE, Harmer J, De Riso A, Timmel CR, Sansom MSP, Berks BC, Schnell JR. 2013. Structural model for the protein-translocating element of the twin-arginine transport system. *PNAS* **110**:E1092–E1101. DOI: https://doi.org/10.1073/pnas.1219486110, PMID: 23471988

Rollauer SE, Tarry MJ, Graham JE, Jääskeläinen M, Jäger F, Johnson S, Krehenbrink M, Liu S-M, Lukey MJ, Marcoux J, McDowell MA, Rodriguez F, Roversi P, Stansfeld PJ, Robinson CV, Sansom MSP, Palmer T, Högbom M, Berks BC, Lea SM. 2012. Structure of the TatC core of the twin-arginine protein transport system. *Nature* **492**:210–214. DOI: https://doi.org/10.1038/nature11683, PMID: 23201679

Rose P, Fröbel J, Graumann PL, Müller M. 2013. Substrate-dependent assembly of the Tat translocase as observed in live *Escherichia coli* cells. *PLOS ONE* **8**:e69488. DOI: https://doi.org/10.1371/journal.pone.0069488, PMID: 23936332

Santini CL, Ize B, Chanal A, Müller M, Giordano G, Wu LF. 1998. A novel sec-independent periplasmic protein translocation pathway in *Escherichia coli*. *The EMBO Journal* **17**:101–112. DOI: https://doi.org/10.1093/emboj/17.1.101, PMID: 9427745

Sargent F, Bogsch EG, Stanley NR, Wexler M, Robinson C, Berks BC, Palmer T. 1998. Overlapping functions of components of a bacterial Sec-independent protein export pathway. *The EMBO Journal* **17**:3640–3650. DOI: https://doi.org/10.1093/emboj/17.13.3640, PMID: 9649434

Sargent F, Stanley NR, Berks BC, Palmer T. 1999. Sec-independent protein translocation in *Escherichia coli*: A distinct and pivotal role for the TatB protein. *The Journal of Biological Chemistry* **274**:36073–36082. DOI: https://doi.org/10.1074/jbc.274.51.36073, PMID: 10593889

Sasaki M, Nishikawa H, Suzuki S, Moser M, Huber M, Sawasato K, Matsubayashi HT, Kumazaki K, Tsukazaki T, Kuruma Y, Nureki O, Ueda T, Nishiyama KI. 2019. The bacterial protein YidC accelerates MPIase-dependent integration of membrane proteins. *The Journal of Biological Chemistry* **294**:18898–18908. DOI: https://doi.org/10.1074/jbc.RA119.011248, PMID: 31662434

Sawasato K, Sato R, Nishikawa H, Iimura N, Kamemoto Y, Fujikawa K, Yamaguchi T, Kuruma Y, Tamura Y, Endo T, Ueda T, Shimamoto K, Nishiyama K-I. 2019a. CdsA is involved in biosynthesis of glycolipid MPIase essential for membrane protein integration in vivo. *Scientific Reports* **9**:1372. DOI: https://doi.org/10.1038/s41598-018-37809-8, PMID: 30718729

Sawasato K, Sekiya Y, Nishiyama KI. 2019b. Two-step induction of cdsA promoters leads to upregulation of the glycolipid MPIase at cold temperature. *FEBS Letters* **593**:1711–1723. DOI: https://doi.org/10.1002/1873-3468.13460, PMID: 31127859

Settles AM, Yonetani A, Baron A, Bush DR, Cline K, Martienssen R. 1997. Sec-independent protein translocation by the maize Hcf106 protein. *Science* **278**:1467–1470. DOI: https://doi.org/10.1126/science.278.5342.1467, PMID: 9367960

Shanmugham A, Wong Fong Sang HW, Bollen YJM, Lill H. 2006. Membrane binding of twin arginine preproteins as an early step in translocation. *Biochemistry* **45**:2243–2249. DOI: https://doi.org/10.1021/bi052188a, PMID: 16475812

Sikdar R, Doerrler WT. 2010. Inefficient Tat-dependent export of periplasmic amidases in an *Escherichia coli* strain with mutations in two DedA family genes. *Journal of Bacteriology* **192**:807–818. DOI: https://doi.org/10.1128/JB.00716-09, PMID: 19880597

Stiegler N, Dalbey RE, Kuhn A. 2011. M13 procoat protein insertion into YidC and SecYEG proteoliposomes and liposomes. *Journal of Molecular Biology* **406**:362–370. DOI: https://doi.org/10.1016/j.jmb.2010.12.036, PMID: 21195087

Suzuki T, Ueno H, Mitome N, Suzuki J, Yoshida M. 2002. F(0) of ATP synthase is a rotary proton channel: Obligatory coupling of proton translocation with rotation of c-subunit ring. *The Journal of Biological Chemistry* **277**:13281–13285. DOI: https://doi.org/10.1074/jbc.M111210200, PMID: 11815616

Tarry MJ, Schäfer E, Chen S, Buchanan G, Greene NP, Lea SM, Palmer T, Saibil HR, Berks BC. 2009. Structural analysis of substrate binding by the TatBC component of the twin-arginine protein transport system. *PNAS* **106**:13284–13289. DOI: https://doi.org/10.1073/pnas.0901566106, PMID: 19666509

Umakoshi M, Hirasawa T, Furusawa C, Takenaka Y, Kikuchi Y, Shimizu H. 2011. Improving protein secretion of a transglutaminase-secreting Corynebacterium glutamicum recombinant strain on the basis of 13C metabolic flux analysis. *Journal of Bioscience and Bioengineering* **112**:595–601. DOI: https://doi.org/10.1016/j.jbiosc.2011.08.011, PMID: 21903468

Walther TH, Grage SL, Roth N, Ulrich AS. 2010. Membrane alignment of the pore-forming component TatA(d) of the twin-arginine translocase from *Bacillus subtilis* resolved by solid-state NMR spectroscopy. *Journal of the American Chemical Society* **132**:15945–15956. DOI: https://doi.org/10.1021/ja106963s, PMID: 20977272

Weiner JH, Bilous PT, Shaw GM, Lubitz SP, Frost L, Thomas GH, Cole JA, Turner RJ. 1998. A novel and ubiquitous system for membrane targeting and secretion of cofactor-containing proteins. *Cell* **93**:93–101. DOI: https://doi.org/10.1016/s0092-8674(00)81149-6, PMID: 9546395

Wu LF, Ize B, Chanal A, Quentin Y, Fichant G. 2000. Bacterial twin-arginine signal peptide-dependent protein translocation pathway: evolution and mechanism. *Journal of Molecular Microbiology and Biotechnology* **2**:179–189 PMID: 10939242.

Yahr TL, Wickner WT. 2001. Functional reconstitution of bacterial Tat translocation in vitro. *The EMBO Journal* **20**:2472–2479. DOI: https://doi.org/10.1093/emboj/20.10.2472, PMID: 11350936

Yen MR, Tseng YH, Nguyen EH, Wu LF, Saier MH. 2002. Sequence and phylogenetic analyses of the twin-arginine targeting (Tat) protein export system. *Archives of Microbiology* **177**:441–450. DOI: https://doi.org/10.1007/s00203-002-0408-4, PMID: 12029389

Zhou W, Hao B, Bricker TM, Theg SM. 2023. A real-time analysis of protein transport via the twin arginine translocation pathway in response to different components of the protonmotive force. *The Journal of Biological Chemistry* **299**:105286. DOI: https://doi.org/10.1016/j.jbc.2023.105286, PMID: 37742925